Plasmonic Nano-lithography For Discreet Media Patterning

L. Pan[1,2] and D. B. Bogy[1,2].

W. Srituravanich[2], Y. Wang[2], C. Sun[2] and X. Zhang[2].

[1] Computer Mechanics Laboratory (CML) of University of California at Berkeley.

[2] NSF Center for Scalable and Integrated NanoManufacturing (SINAM).

Abstract

The development of the hard disk drive industry demands 10 Tbpsi recording density which leads to the implementation of patterned media. Making patterned media requires the development of high-throughput nano-fabrication technologies. Conventional nanolithography techniques, such as electron-beam and scanning probe lithography, are limited by their low throughput and high cost. Here we report a new low-cost high-throughput approach to maskless nanolithography that uses an array of plasmonic lenses that "flies" above the surface to be patterned, concentrating short wavelength surface plasmons into sub wavelength spots. However, these nanoscale spots are only formed in the near field, which makes it very difficult to scan the array above the surface at high speed. To overcome this problem we have designed a self-spacing air-bearing surface that can fly the array just 20 nm above a disk that is spinning at speeds of 4-12 meter/second, and we have experimentally demonstrated patterning with a linewidth of 80 nm. Theoretical simulation, however predicts 5-10nm resolution using this approach. This low-cost nano-fabrication scheme has the potential to achieve throughputs that are two to five orders of magnitude higher than other maskless techniques.

1 Introduction

During the past decade, areal density in hard disk drives has doubled almost every 18 months. In order to keep increasing the areal density up to 10 Tbpsi according to the industry roadmap, researchers are considering patterned media, where the bits are magnetically separated from each other. This approach offers the possibility to solve the issue of the superparamagnetic limit caused by the thermal instability of too closely spaced magnetic bits. The most challenging part for the implementation of patterned media is the making the media itself. At 10 Tbpsi, the minimum feature size is below 10 nm, which is beyond the capability of conventional optical lithography[1, 2] according to their roadmap. Although nano-imprint lithography (NIL) can meet most of the needs of HDD as compared to conventional lithography including focused ion-beam[3], scanning-probe lithography[4-6] (SPL) and electron-beam[7], it relies on other tools to make the 1X imprint masters. Even though many methods can provide sub 10 nm resolutions, the low throughput of these methods due to the serial and slow scanning nature remains the bottleneck. Although multi-axial electron-beam lithography[8-10] has been proposed to increase throughput by using multiple electron beams in parallel, the difficulties for simultaneously regulating the multiple beam sizes and beam positions because of the thermal drift and electrical charge Coulomb interactions that result in significant lens aberration make its future uncertain. Zone-plate-array lithography[11] (ZPAL), utilizes a large array of diffractive optical elements or spatial light modulators to improve the throughput, but the ultimate resolution is still restricted to the diffraction limit. Scanning-probe lithography (SPL), a tip-based low-cost alternative operating in ambient environment, has made a noticeable throughput improvement, as shown in a recent demonstration using 55,000 probes scanning at the speed of 60 μm/s[12]. Its throughput is still two to three orders of magnitude lower than that required by practical nano-fabrication applications[13]. This is because SPL technology, which relies on the slow scan of the tips at 10-100 nm from the surface, has limited feedback bandwidth to control the tip-sample distance at higher speed. We report here a novel high-throughput plasmonic nanolithography to circumvent

the critical parallelization and slow scanning challenges which can potentially increase the throughput by two to five orders of magnitude compared to that achieved by parallel SPL and commercial electron beam lithography.

2 Plasmonic Lens and Head Design and Fabrication

Surface plasmons (surface plasmon polaritons) (SPPs) are known as the collective oscillation of electrons at a metal-dielectric interface[14-16]. SPPs can have much shorter wavelengths than the light propagating in free space, and therefore it is promising for new applications for imaging[17] and lithography[18-20] with resolution below the diffraction limit. A plasmonic lens made of a concentric ring grating has been used to focus the light to a sub-100 nm spot at the near field with local intensity more than 100 times higher than the incident light[21]. These earlier results clearly suggest the potential of using plasmonic lens for nanolithography. However, due to the exponential decay of the evanescent field, the tightly focused spot only exists at the near field of the plasmonic lens, normally closer than 100 nm. Thus, high throughput nano-patterning requires some new mechanism to ensure precise control of the nano-scale gap between the plasmonic lens and substrate during high-speed writing.

We report here the first high-speed flying plasmonic lens arrays using an air bearing (Fig. 1). To achieve high-speed scanning while maintaining the nano-scale gap, we designed a novel air-bearing slider to fly the plasmonic lens arrays at the height of 20 nm above the substrate at speeds of 4-12 meter/second. The rotation of the substrate creates an air flow along the bottom surface of the plasmonic flying head, known as the air bearing surface (ABS). The ABS generates an aerodynamic lift force and it is balanced by the force supplied by the suspension arm to precisely regulate a nano-scale gap between the plasmonic lens arrays and the rotating substrate, which is covered with photoresist. With the high bearing stiffness and small actuation mass, this self-adaptive method can provide an effective bandwidth

up to 120 kHz. The usage of such an ABS eliminates the need for a feedback control loop, and therefore it overcomes the major technical barrier for high-speed scanning. As shown in Figure 1, the high-throughput nano-lithography is accomplished using the plasmonic flying head at a relatively high speed. The plasmonic flying head is made of a specially designed transparent air bearing slider with arrays of plasmonic lenses fabricated on its surface adjacent to the disk. Employing large arrays of plasmonic lenses enables the parallel writing necessary for high throughput.

In this work, the plasmonic flying heads were fabricated using micro-fabrication techniques and focused ion beam, and they were evaluated using a dynamic flying height tester (DFHT IV, Phase Metrics). The plasmonic lens was numerically designed and simulated with the result showing an intensity enhancement factor of 100 times and the focused spot of 80 nm as shown in Figures 2a and 2b. Considering a focal spot within 10% variation as a criterion, numerical simulation shows that a flying height within the range from 0 to 30 nm is acceptable. Given this, the parallelism between the plasmonic lens array and substrate needs to be carefully considered in designing ABS, which was accomplished using in-house developed air bearing simulators *CMLair*[22]. The goal was to achieve a consistent flying height of 20 nm at scanning speeds from 4 to 12 m/s considering the fact that the disk linear velocity reduces and the skew angle changes as the slider goes from the outer to inner radius. Figures 2c, 2d show the air bearing surface design and a simulated air bearing pressure profile. The ABS design consists of a four-pad U-shaped dual-rail with a long front bar (Fig. 2c). Two large rear pads generate the repelling peak pressure to float the flying head and prevent possible physical contacts (Fig. 2d). The two front pads produce the steering repelling pressure to increase the bearing roll stiffness and minimize the roll angle. A sub-2 μrad roll angle is achieved across the disk by adjusting the detailed shape and depth of the rail and pads. The pitch angle is designed to be around 80 μrad rather than even smaller to compensate for the curvature variations of both the slider and disk. By throttling injecting air from the leading edge, the long-bar design can significantly

reduce the slider's pitch angle, contamination sensitivities and also enhance the slider's damping. The U-shaped dual-rail design efficiently increases the overall sub-ambient ("negative") pressure which improves both the slider's stability and bearing stiffness. As the disk velocity decreases, both the positive pressure and negative pressure decrease, which results in lower flying height and bearing stiffness. The effective air bearing stiffness and damping ratio are about 2×10^5 N/m and 0.1 respectively. The design provides about 85 kHz effective bandwidth for gap control. The flying plasmonic lens array in the optical near field is inspired by the magnetic recording head in hard disk drives (HDD). Unlike a conventional HDD ABS[23] which uses only the trailing edge mounted transducer to serially read and write the magnetic bits, we designed the plasmonic head to contain a relatively large area filled by plasmonic lenses that enable the parallel writing and high throughput. Due the to rapid decay of the light intensity of plasmonic lens, all plasmonic lenses need to keep a distance to the rotating substrate within 30nm, which requires the bottom surface to be parallel to the substrate to within 100 μrad tilt. This stringent parallelism requirement made the design of the plasmonic head very challenging and different from magnetic head sliders. For example, to fly 1,000 lenses within the 30 nm gap tolerance over the usable area of 800 μm × 20 μm on the rear pads with each plasmonic lens size 4 μm in diameter, the ABS needs to be designed with less than 100 μrad pitch angle and 2 μrad roll angle. Also, the ABS needs a larger air bearing stiffness, higher damping ratio and better contamination insensitivity than conventional ABS. In addition, the plasmonic head must be transparent to light.

Figure 3a shows an optical microscope image of the fabricated plasmonic flying head where the sapphire ABS coated with a metal film was assembled to the suspension, and a SEM image of a 2-D array of plasmonic lenses (4x4) fabricated on the ABS in a square lattice (Fig. 3b). Figures 3c, d show the fly height and pitch and roll angle measurements together with simulation results. We observed that the flying height is uniform over the velocity range 4 to 12 m/s. The measured flying height is in good agreement with the simulated ABS design performance with slight

variation from 18.0 nm to 20.4 nm, which is within the tolerance of 30 nm (Fig. 3c). The parallelism of the ABS is determined by the roll and pitch angles of the ABS with respect to the substrate. Under the above linear velocity range, the experimental measured roll and pitch angles vary from 0.15 μrad to -2.34 μrad and 61 μrad to 89 μrad, respectively, in good agreement with simulation design, which ensures the entire 1,000 lens array is within the 30nm gap tolerance.

3 Experimental Results and Future Work

In the lithography experiment, A UV CW laser was focused down to a several micrometer spot onto a plasmonic lens which further focused the beam to a sub-100 nm spot onto the spinning disk for writing of arbitrary patterns (Fig. 1c). The laser pulses are controlled by an electro-optic modulator according to the signals from a pattern generator. The writing position is referred to the angular position of the disk from the spindle encoder and the position of a piezo-stage along the radial direction. We use an inorganic TeO_x based thermal photoresist[24] deposited on a glass disk by magnetic sputtering. A spindle was used to rotate the 4-inch diameter disk at 2,000 rpm which is equivalent to the linear speed of 10 m/s at the outer radius. After pattern writing and development in diluted KOH solution, the patterns were examined using an atomic force microscope. The result demonstrated that we can achieve high-speed patterning with 80 nm line widths at 10 m/s (Fig. 4a). Figures 4b and c demonstrate successful patterning of arrays of the acronym “SINAM” with the feature size of 145 nm. The resolution can be improved by careful design using shorter plasmon wavelength and guiding mechanisms, and theoretical simulation shows it can reach down to 5-10 nm[25]. Due to the fast scanning, a single plasmonic lens already has higher throughput than most other maskless lithography approaches. The throughput of plasmonic nanolithography can be greatly enhanced by employing a larger number of plasmonic lenses for parallel writing. For example, consider a 1,000 lenses array occupying the area of 800 μm × 20 μm at the bottom of the ABS with each plasmonic lens having a 4 μm in diameter. Taking

into account the changes of the mean flying height, as well as pitch and roll angles at different linear velocities, our simulation shows that the corresponding flying height variation for all the plasmonic lenses is in the range from 18 to 24 nm, which is well within the acceptable range of 0-30nm. Thus, at the scanning speed of 10 m/s, a plasmonic flying head carrying 1000 lenses can write a 12" wafer in 2 minutes. Furthermore, a slider of a few millimetres in size may take up to 10^5 lenses. Flying plasmonic lens arrays at optical near field enables the agile maskless nano-scale fabrication with the potential of two to five orders of magnitude higher throughput than conventional maskless techniques. In future industrial implantation of this technology, engineering challenges must be addressed such as pattern data management, lithography linewidth control, pattern overlay and resist defect reduction, which are common for all maskless lithography approaches. Integrated approaches for precision engineering, metrology, as well as new resist development will be needed. This high-speed technique can also be used for nano-scale metrology and imaging. Such a low cost, high-throughput scheme promises a new route towards the next generation of nano-manufacturing.

Acknowledgments

The authors are grateful to Zhaowei Liu and Dongmin Wu for the helpful discussions. This work was financially supported by the NSF Center for Scalable and Integrated NanoManufacturing (SINAM) (Grant # DMI-0327077) and in collaboration with Computer Mechanics Laboratory (CML) of University of California at Berkeley.

References

1. Okazaki, S. Resolution limits of optical lithography. *J. Vac. Sci. Tech. B* **9**, 2829-2833 (1991).

2. Jeong, H. J. *et al.* The future of optical lithography. *Solid State Technol.* **37**, 39-47 (1994).

3. Melngailis, J. Focused ion-beam technology and applications. *J. Vac. Sci. Tech. B* **5**, 469-495 (1987).

4. Cooper, E. B. *et al*. Terabit-per-square-inch data storage with the atomic force microscope. *Appl. Phys. Lett.* **75**, 3566-3568 (1999).

5. Piner, R. D., Zhu, J., Xu, F., Hong, S. & Mirkin, C. A. "Dip-pen" nanolithography. *Science* **283**, 661-663 (1999).

6. Vettiger, P. *et al*. The "Millipede" - more than one thousand tips for future AFM data storage. *IBM J. Res. Develop.* **44**, 323–340 (2000).

7. Groves, T. R. & Kendall, R. A. Distributed, multiple variable shaped electron beam column for high throughput maskless lithography. *J. Vac. Sci. Tech. B* **16**, 3168-3173 (1998).

8. McCord, M. A. Electron beam lithography for 0.13 μm manufacturing. *J. Vac. Sci. Tech. B* **15**, 2125-2129 (1997).

9. Muraki, M. & Gotoh, S. New concept for high-throughput multielectron beam direct write system. *J. Vac. Sci. Tech. B* **18**, 3061-3066 (2000).

10. Pease, R. F. *et al.* Prospect of charged particle lithography as a manufacturing technology. *Microelectron. Eng.* **53**, 55–60 (2000).

11. Menon, R., Patel, A., Gil, D., & Smith, H. I. Maskless lithography. *Materials today* **8**, 26-33 (February 2005).

12. Salaita, K. *et al*. Massively parallel dip-pen nanolithography with 55,000-pen two-dimensional arrays. *Angew. Chem. Int. Edn* **45**, 7220-7223 (2006).

13. Pease, R. F. Maskless lithography. *Microelectron. Eng.* **78-79**, 381-392 (2005).

14. Ritchie, R. H. Plasma losses by fast electrons in thin films. *Phys. Rev.* **106**, 874–881 (1957).

15. Barnes, W. L., Dereux, A., & Ebbesen, T. W. Surface plasmon subwavelength optics. *Nature* **424**, 824 - 830 (2003).

16. Genet, C. & Ebbesen T. W. Light in tiny holes. *Nature* **445**, 39 - 46 (2007).

17. Fang, N., Lee, H., Sun, C. & Zhang, X. Sub-diffraction-limited optical imaging with a silver superlens. *Science* **308**, 534-537 (2005).

18. Srituravanich, W., Fang, N., Sun, C., Luo, Q. & Zhang, X. Plasmonic nanolithography. *Nano Letters* **4**, 1085-1088 (2004).

19. Luo, X. & Ishihara, T. Surface plasmon resonant interference nanolithography technique. *Appl. Phys. Lett.* **84**, 4780-4782 (2004).

20. Liu, Z. *et al*. Focusing surface plasmons with a plasmonic lens. *Nano Letters* **5**, 1726-1729 (2005).

21. Ozbay, E. Plasmonics: Merging photonics and electronics at nanoscale dimensions. *Science* **311**, 189-193 (2006).

22. Juang, J., Bogy, D. B., & Bhatia, C. S. Design and dynamics of flying height control slider with piezoelectric nanoactuator in hard disk drives. *ASME J. Tribol*. **129**, 161-170 (2007).

23. Han, Y., Liu, B., & Huang, X. High air-bearing stiffness slider design. *J. Magn. Magn. Mater*. **303**, e76-e80 (2006).

24. Ito, E., Kawaguchi, Y., Tomiyama, M., Abe, S. & Ohno, E. TeO_X-based film for heat-mode inorganic photoresist mastering. *Jpn. J. Appl. Phys.* **44**, 3574-3577 (2005).

25. Stockman, M. I. Nanofocusing of optical energy in tapered plasmonic waveguides. *Phys. Rev. Lett.* **93**, 137404 (2004).

Figures

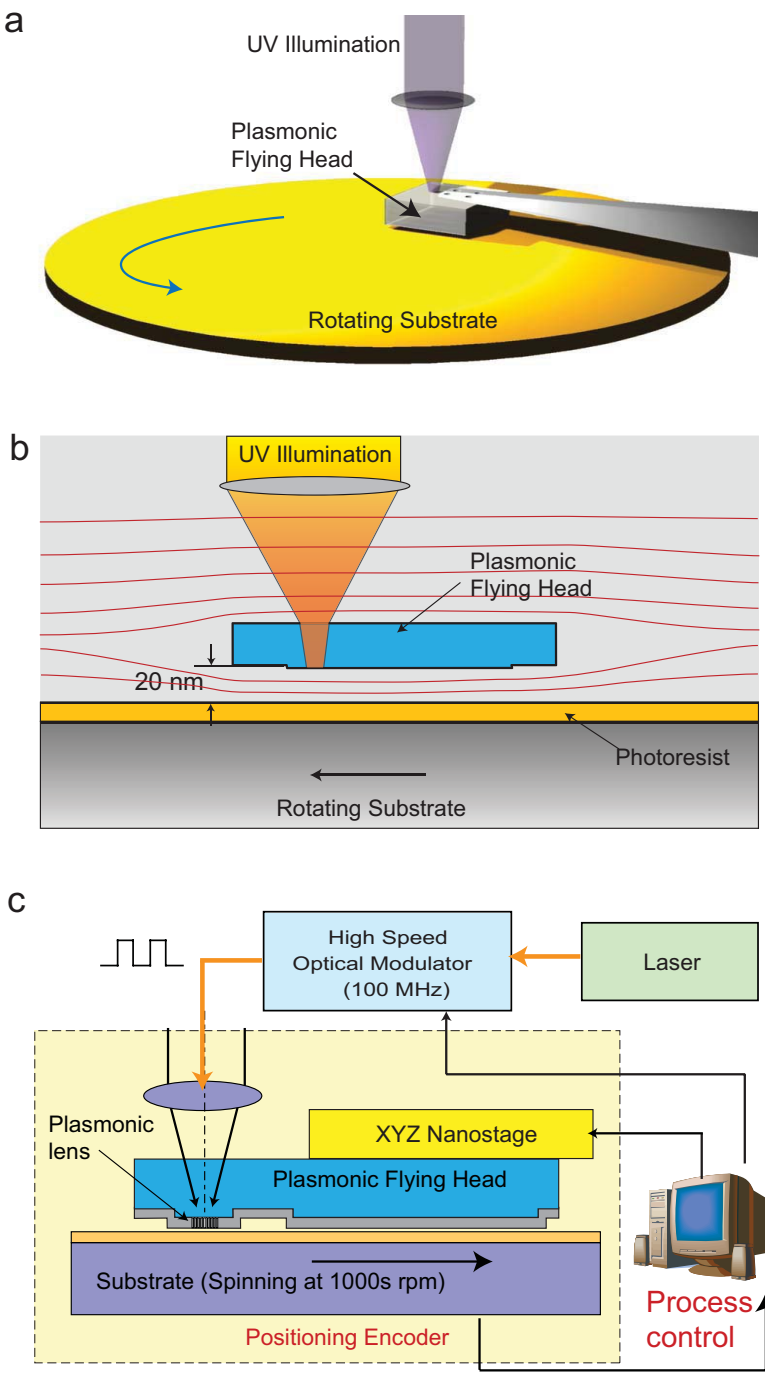
a
UV Illumination
Plasmonic
Flying Head
Rotating Substrate
b
UV Illumination
Plasmonic
Flying Head
20 nm
Photoresist
Rotating Substrate
c
High Speed
Optical Modulator
(100 MHz)
Laser
Plasmonic
lens
XYZ Nanostage
Plasmonic Flying Head
Substrate (Spinning at 1000s rpm)
Positioning Encoder
Process
control

Figure 1. High-throughput maskless nanolithography using plasmonic lens arrays. (a) Schematic showing the lens array focusing ultraviolet (365 nm) laser pulses onto the rotating substrate to concentrate surface plasmons into sub-100 nm spots (top). However, sub-100 nm spots are only produced in the near field of the lens, so a process control system (bottom) is needed to maintain the gap between the lens and the substrate at 20 nm (middle).

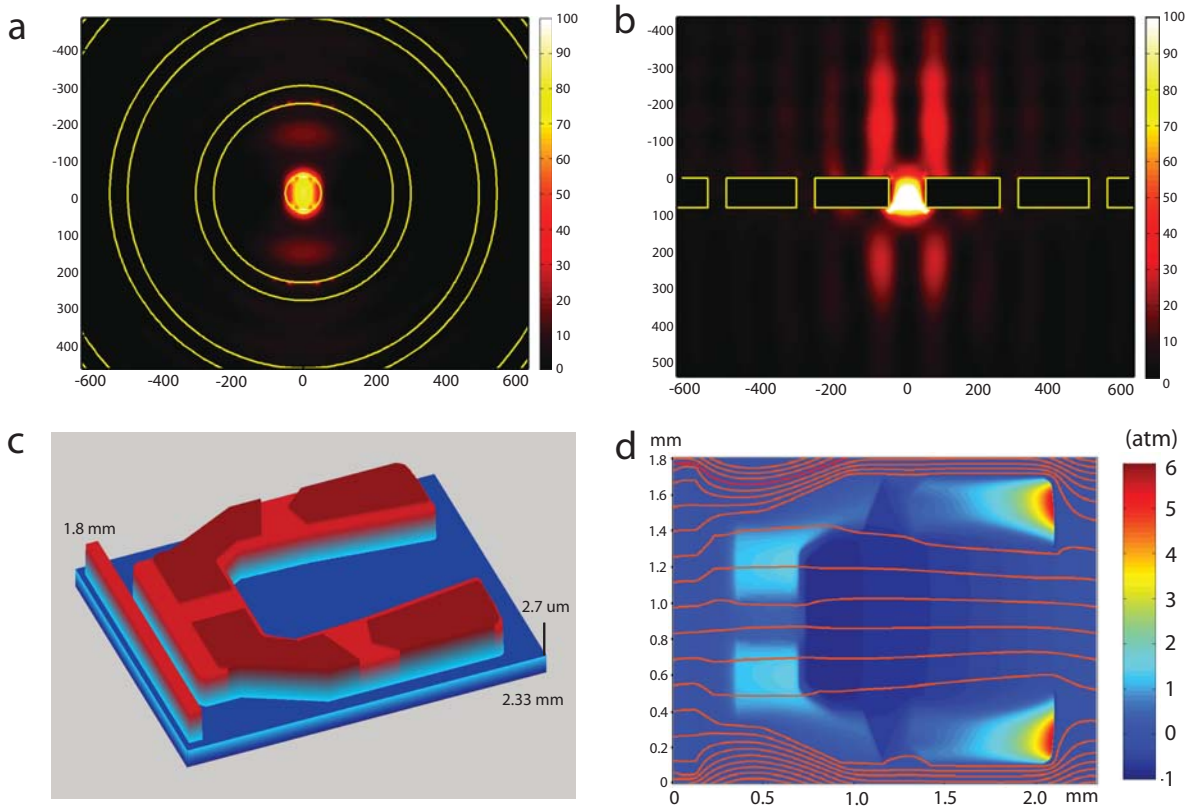

Figure 2. Designs and simulations for plasmonic lens and air bearing surface (ABS). (a) Plasmonic lens is made of a nano-aperture surrounded by 15 through rings on an aluminium film; calculated intensity at 20 nm away from the lens under the linearly polarized light illumination at the wavelength of 365 nm. A tightly focused 80 nm spot can be obtained in the near field. The aperture diameter, ring periodicity, ring width and aluminium layer thickness are 100, 250, 50 and 80 nm, respectively. (b) Cross section view of the plasmonic lens and the intensity enhanced about 100 times at the focal point compared to that of the incident light. (c) ABS with oblique view. The topography is scaled up by 200 times for better illustration. The ABS generates an aerodynamic lift force and it is balanced with the force supplied by suspension to precisely retain a nano-scale gap between the plasmonic lens arrays and the rotating substrate. (d) Calculated normal air pressure (colored) and air-mass flow lines (from left to right) under the ABS with the scanning speed at 10 m/s. The pressure is

normalized to ambient air pressure. The mass flow lines density is proportional to the mass flow. At the lowest point, the air pressure is maximized but the mass flow is minimized which favours both air bearing stiffness and contamination tolerance.

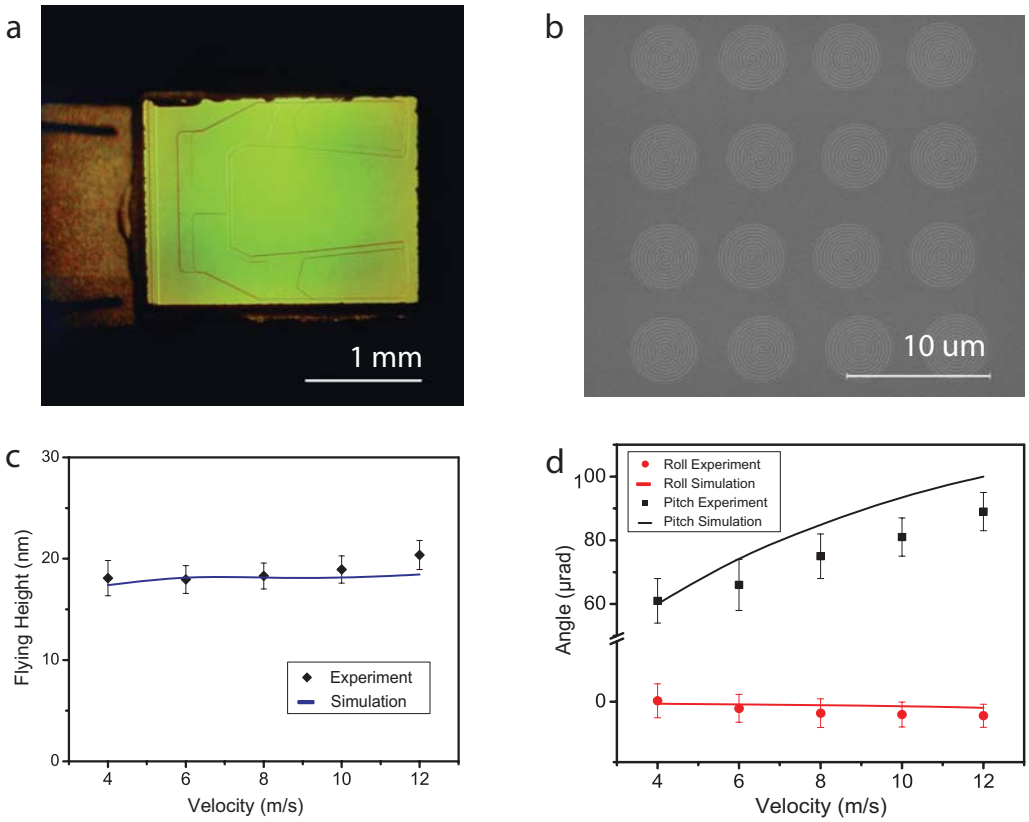

Figure 3. Fabricated plasmonic flying head and flying height measurement. (a) Optical micrograph of a plasmonic flying head assembled with suspension. (b) SEM image of array of plasmonic lenses fabricated on an air bearing surface. (c) Measured and calculated flying height shows the slider maintains the flying height at 20±2 nm, with the scanning speeds from 4 to 12 meter/second. (d) Measured and simulated pitch and roll angle at the scanning speeds from 4 to 12 meter/second. Agreement between experiment and the simulation demonstrates the parallelism achieved is within the gap tolerance of 30 nm over the whole area of plasmonic lens array and the substrate.

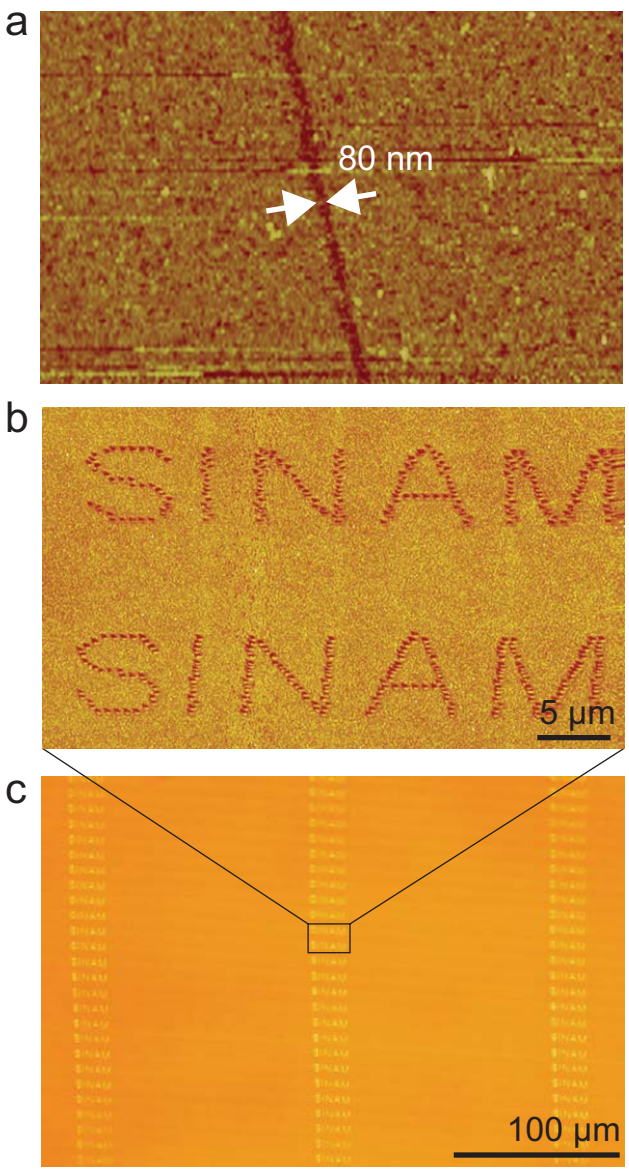

Figure 4. Maskless Lithography by flying plasmonic lenses at near field. (a) AFM image of pattern with 80 nm line width on the TeO_x based thermal photoresist. (b) AFM image of arbitrary writing of “SINAM” with 145 nm line width. (c) Optical micrograph of patterning of the large arrays of “SINAM”.